Lab on a Chip

COMMUNICATION

View Article Online
View Journal | View Issue

Cite this: *Lab Chip*, 2019, **19**, 1327

Received 22nd January 2019,
Accepted 14th March 2019

DOI: 10.1039/c9lc00070d

rsc.li/loc

Waveguide-based chemo- and biosensors: complex emulsions for the detection of caffeine and proteins†

Lukas Zeininger, Elisabeth Weyandt, Suchol Savagatrup, Kent S. Harvey, Qifan Zhang, Yanchuan Zhao and Timothy M. Swager *

We report on a new modular sensing approach in which complex emulsions serve as efficient transducers in optical evanescent field-based sensing devices. Specifically, we leverage the tunable refractive index upon chemically triggered changes in droplet morphology or orientation. Variations in the optical coupling result in readily detectable changes in the light transmitted from a waveguide.

Optical waveguide-based sensing devices offer sensitive, non-invasive, and label-free detection of chemical and biological analytes with near real-time responses.[1,2] Waveguide technologies exploit direct or indirect evanescent wave interactions with an analyte. Specifically, an evanescent field is coupled into a thin optically transparent film, and the degree to which the light is out-coupled from the waveguide is dependent upon the refractive index of the sample.[3] The amplitude of the evanescent field decreases exponentially with distance from the surface with a penetration depth, typically of about 200 nm, which allows for sensing interactions with the environment immediately surrounding the waveguide.[4] Evanescent field sensing has been widely used in devices targeting physical,[5] chemical,[6] or biological events[7] by detecting changes in evanescent fluorescence,[8] refractive index,[9] or spectroscopic shifts.[10,11] Popular examples include waveguide sensors for the detection of pathogens,[12,13] total internal reflection fluorescence spectroscopy and dual-polarization interferometry,[14,15] as well as fingerprint identification scanners.[16] Realizing broader practical applications of waveguide-based chemo- and bio-sensors requires improved concepts for the reproducible, versatile, and cost-effective fabrication of modular sensing platforms that allow for enhanced signals upon chemical recognition of an analyte.[17,18]

Department of Chemistry and Institute for Soldier Nanotechnologies, Massachusetts Institute of Technology, Cambridge, MA 02139, USA. E-mail: tswager@mit.edu

† Electronic supplementary information (ESI) available: Materials and methods, experimental details, synthetic procedures, and additional sensing experiments. See DOI: 10.1039/c9lc00070d

Traditional waveguide-based chemo- and biosensors primarily detect the interactions of analytes with immobilized selectors at the interface of the waveguide.[19] The covalent or physical immobilization of transducers on waveguide surfaces poses a challenge in creating reproducible and ultrasensitive sensor devices with uniform and consistent sensing area. In addition, the sensitivity can be severely reduced if changes in refractive index upon binding of an analyte onto the waveguide surface are minor. To this end, molecular sensing layers have been developed that impart colorimetric or fluorometric responses to facilitate transduction of the signal.[20] However, in these approaches, high concentrations of analytes are required to obtain detectable signals within the small penetration depth of the evanescent field. More recently, significant advancements have been made in the development of new refractive index sensing device technologies, including plasmonic resonators,[21,22] spiral waveguides,[23] optical fibers,[24–26] and resonant microcavities.[27–29] These devices have been shown to impart exceptional sensitivity, yet, practical applications are hindered by complications including a challenging replication of robust instrumental platforms, incapability to produce real-time and multiplexed signals, or expensive and complicated manufacturing.

We report herein a new modular sensing approach in which multicomponent oil-in-water emulsions serve as transduction materials in optical waveguide-based sensors. Specifically, we leverage the tunable refractive index of the emulsions upon chemically triggered changes in droplet morphology to manipulate the out-coupling of light (Fig. 1).

Light propagating through a glass waveguide will undergo total internal reflection (TIR) at the interface when in contact with low refractive index media (*i.e.*, air, water, fluorocarbon). However, if a higher refractive index organic solvent is proximate to the interface, an out-coupling of light from the waveguide is realized. As a result, functional surfactants that trigger changes in droplet morphology and symmetry in response to external stimuli can be used to modulate the out-coupling of light. Thus, dynamic complex emulsions with

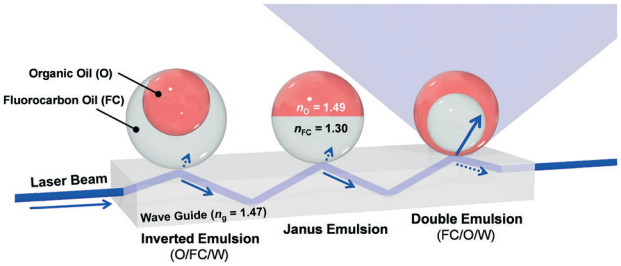

Fig. 1 Conceptual sketch of the modular sensing approach consisting of dynamic complex emulsions in three different morphologies on top of a waveguide-based sensing device. Beginning on the left, total internal reflection (TIR) is observed for inverted and Janus emulsions. Upon transition to a double emulsion with the higher index organic phase on the outside, the laser light is out-coupled from the waveguide, thereby increasing light intensity measured above the waveguide.

functional surfactants can be used to amplify signals and broaden the scope of waveguide-based sensing devices.

The transduction in Fig. 1 requires multicomponent emulsions with a dynamic morphology that are dispersed within a continuous phase. To this end, we prepared double emulsions containing dibutyl phthalate (n_O = 1.49) as the higher refractive index liquid and methoxyperfluorobutane (n_{FC} = 1.30) as the lower index liquid. The emulsions are produced by a microfluidic device using a temperature-induced phase-separation approach.[30] Briefly, the two liquids were heated above their critical solution temperature (T_c = 28 °C) and emulsified in an aqueous continuous phase containing organic and/or fluorocarbon surfactants. Upon cooling, phase separation gave rise to structured emulsions with a uniform morphology that is determined by the balance of the organic/water and fluorocarbon/water interfacial tensions. Furthermore, the morphology of these complex emulsions can be dynamically alternated between inverted (O/FC/W), Janus, and double (FC/O/W) emulsions by varying the interfacial tensions.[30] We then fabricated a sensitive optical read-out capable of detecting small morphological changes by placing as-prepared double emulsions onto the surface of a right-angle glass prism (Fig. 2A). The droplets aligned by the gravitational force and assembled into a highly reproducible densely packed monolayer on the glass surface. A laser beam (λ = 405 nm), directed into the glass prism (n_g = 1.47) at an angle above the critical angle (Θ_c = arcsin (n_w/n_g)), resulted in TIR at the interface containing the droplets and the aqueous surfactant solution (n_W= 1.33). We incorporated an emissive dye (perylene) into the organic phase to differentiate the out-coupled light (λ = 475 nm) and the background stray light. The intensity of this emission was then measured normal to the surface of the complex emulsions.

We first validated our sensing scheme by measuring the intensity of the out-coupled light as a function of the droplet morphologies as controlled by the ratio of commercial organic and fluorocarbon surfactants, sodium dodecyl sulfate (SDS) and Zonyl FS-300 (Zonyl). We used the ratio of the two surfactant fractions (f_{Zonyl}/f_{SDS} or $f_{Zonyl}/1\text{-}f_{Zonyl}$) as a metric of droplet morphologies. Specifically, we obtained double emulsions (FC/O/W) when f_{Zonyl} is 0 ($f_{Zonyl}/1\text{-}f_{Zonyl}$ = 0) and Janus

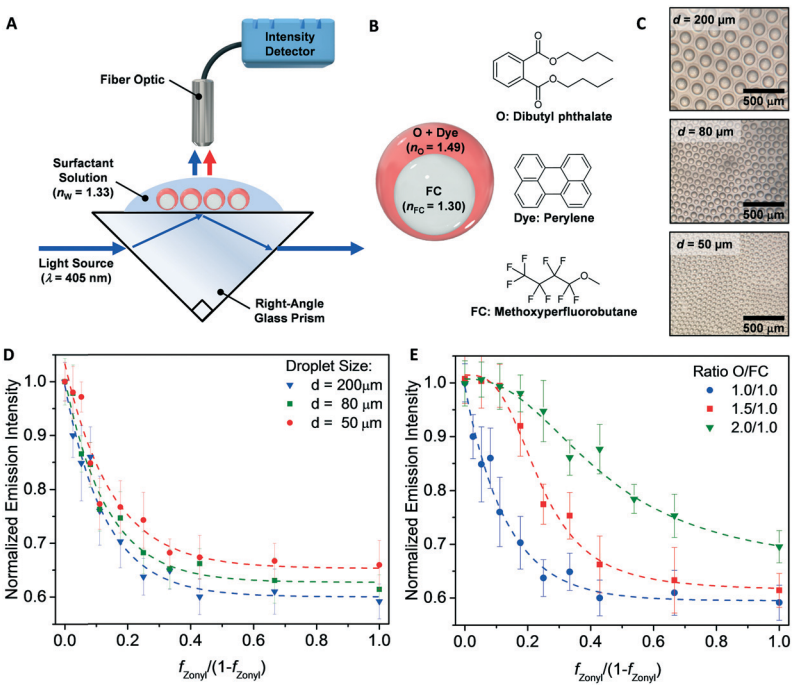

Fig. 2 Waveguide-based sensing device and optical read-out of changes in droplet morphology. (A) Schematic illustration of the measurement system and (B) chemical structures of the complex emulsions. (C) Optical micrographs of monodisperse double-phase emulsions with varying diameters on top of the right-angle glass prism. Measured light intensity of complex emulsions as a function of different morphologies for three different droplet sizes with 1 : 1 O/FC ratio (D) and for droplets with differing O : FC ratios with diameter of 200 μm (E) ($N \geq 5$ measurements).

emulsions when f_{Zonyl} is 0.5 ($f_{Zonyl}/1\text{-}f_{Zonyl}$ = 1). As expected, we recorded the highest emission for double emulsions with the high refractive index organic phase proximate to the glass prism. With increasing f_{Zonyl}, we observed a rapid decrease in light intensity as the morphology shifted from double emulsions to Janus emulsions. This trend was observed for complex emulsions of three different diameters (50, 80, and 200 μm) with minimal variation (Fig. 2D). We attributed this observation to the relatively small evanescent field penetration depth in comparison to the size of the emulsions. However, we observed shifts in the onset of the intensity decay when we varied the volume ratio between the organic and fluorocarbon oils (Fig. 2E). For droplets with an O : FC ratio of 1.5 : 1 and 2 : 1, the organic phase coupled to the evanescent wave over a greater range of morphology.

To demonstrate this waveguide-based sensing paradigm, we have devised a scheme for the rapid and sensitive detection of caffeine. Caffeine represents an extensively studied target in molecular recognition and development of chemical sensors,[31,32] however there remains a need for inexpensive portable devices to quantify caffeine in complex mixtures. To transduce caffeine recognition using complex emulsions, we synthesized a caffeine-responsive surfactant, inspired by a previously reported palladium pincer complex that binds caffeine in complex matrices.[33] This adaptation involved creating an amphiphilic Pd-pincer complex $C_{10}P$ 9 containing two hydrophilic glycol chains and one hydrophobic aliphatic moiety. The synthesis of the Pd-pincer complex began with chelidonic acid 1 (Fig. 3A) and its conversion to chlidamic acid 2. The aliphatic decyl moiety was attached by Williamson ether and the tetraethylene glycol moieties were attached *via* amide-bond formation between 4-(decyloxy)-pyridine-2,6-dicarbonyl dichloride 6 and 4-((2,5,8,11-tetraoxatridecan-13-yl)oxy)aniline 7. Inserting the Pd-center produces $C_{10}P$ 9, which proved to be an effective surfactant for stabilizing organic emulsions in water even at low concentrations (<1 wt%). Functional complex emulsions were prepared by substituting SDS with $C_{10}P$ and the ratio of $C_{10}P$: Zonyl similarly determines the droplet morphology. Measurements of the light intensity above droplet layers on the waveguide device resulted in the characteristic behavior, demonstrating the effectiveness of $C_{10}P$ as a surfactant (Fig. 3B).

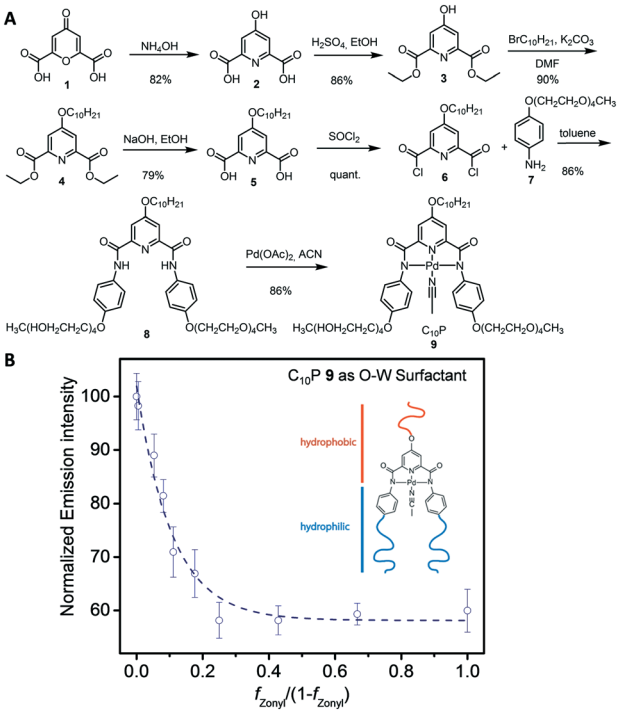

Fig. 3 (A) Synthesis of the Pd-pincer surfactant $C_{10}P$ 9. (B) Light intensity read-out of emulsions formed from varying ratios of $C_{10}P$ and Zonyl with diameters of 200 μm, $N \geq 5$ measurements.

The resulting stimuli-responsive $C_{10}P$ surfactant binds caffeine in its hydrophobic binding pocket at the droplet interface, resulting in an increase of hydrophobicity and a decrease in its surfactant strength. As a result, small amounts of caffeine can produce changes in the droplet morphology. We have shown previously that double and inverted emulsions induce optical scattering and obscure optical transmission, while Janus emulsions appear transparent.[34] Thus, as a qualitative demonstration, we observed this transition from a transmissive state to an opaque state when caffeine is added to Janus droplets stabilized with $C_{10}P$ and Zonyl surfactants (Figure S1†). For a more quantitative demonstration, we analyzed the optical micrographs of the emulsions using image processing software to track the droplet morphologies at each concentration of caffeine (Figure S2†). As expected, a stepwise addition of caffeine to the solution of $C_{10}P$ and Zonyl surfactants reduced the surfactant strength of $C_{10}P$ and decreased the organic-water interfacial area.

After the validation of the interaction between $C_{10}P$-functionalized emulsions and caffeine, a rapid quantitative readout was realized by depositing the complex emulsions (ratio of $C_{10}P$: Zonyl surfactants: 95 : 5) onto the waveguide-based sensor. Upon the addition of caffeine, the change in morphology from a nearly encapsulated double emulsion towards Janus state was monitored by recording the decrease in light intensity, measured above the droplet layer. For low caffeine concentrations, the calibration curve was relatively linear (R^2 = 0.99) and allowed for the detection of caffeine in the concentration range between 0.1 to 0.5 mM (Fig. 4A). Notably, the precision of our method can be tuned by varying the surfactant concentration in solution. Specifically, a decrease of the overall surfactant concentration from 1 wt% to 0.1 wt% resulted in a sensitivity increase and a precise detection (R^2 = 0.98) of caffeine in the micromolar range (Fig. 4B).

In addition, dynamic interactions between multiple droplets also offer opportunities in waveguide-based sensors. In particular, we have determined that a triggered tilting of Janus droplets can produce efficient optical out-coupling of light. We have previously demonstrated that the agglutination of particles can be evoked by multivalent binding units (Fig. 5A and B), such as proteins and bacteria.[35] Janus droplets, naturally aligned by gravity with the lower density organic phase on the upward side, can be trapped in tilted

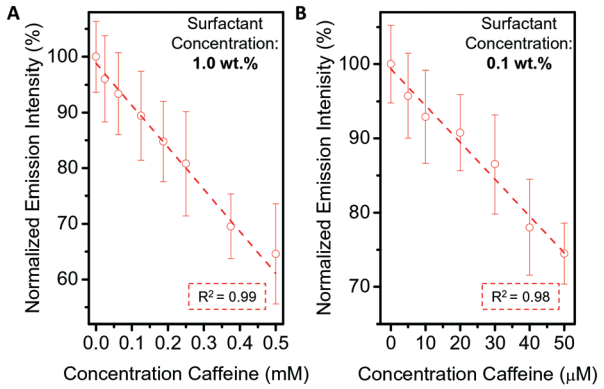

Fig. 4 Sensing of caffeine using the waveguide-based sensing device. The sensitivity can be fine-tuned through variations of the overall surfactant concentration in solution. Emission intensity decrease as a function of caffeine concentration for emulsions in a (A) 1.0 wt% and (B) 0.1 wt% surfactant solution (ratio of $C_{10}P$: Zonyl surfactants: 95 : 5).

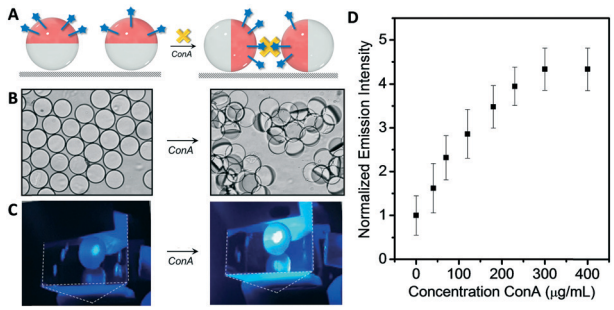

Fig. 5 Optical detection of droplet agglutination (A) droplet tilting scheme and (B) optical micrograph of Janus droplet monolayers before and after agglutination. (C) Images of Janus droplets on top the waveguide device taken before and after droplet agglutination. (D) Quantitative optical read-out of the light intensity measured as a function of the concentration of concanavalin A (ConA) ($N \geq 5$ measurements).

organizations by multiple host-guest binding interactions between functional surfactants and an analyte. For example, mannose-functionalized droplets can bind to concanavalin A (ConA), a sugar-binding lectin that serves as mimic for the foodborne pathogen *E. coli*.[36] Similarly to the above described optical read-out for morphology changes, the tilting of Janus droplets led to a decrease of the distance between the high-refractive index organic phase and the glass surface. As a result, an increase of the light intensity normal to the surface containing the droplets was detected (Fig. 5C and D). We attributed the sensitivity in this scheme to a higher excitation light intensity entering the droplets as a result of the larger interface between the glass slide and the O-phase as well as favorable angle distribution in which light rays can enter the droplets. As a result, a pronounced increase of the light intensity was measured above the agglutinated droplet samples with an up to almost 5-fold increase of the measured light intensity for fully agglutinated samples. Thus, besides innovations in the interfacial recognition that allow for the implementation of molecular sensors with limited utility in native aqueous biosensing conditions, the dynamic nature of complex double emulsions offers the possibility to create large refractive index changes within the evanescent field region of waveguide sensing devices.

Conclusions

A new modular sensing approach with the potential to enhance the sensitivity and reproducibility of new and existing waveguide-based sensing devices is reported. The transduction units, complex organic/fluorocarbon/water (O/FC/W) emulsions constitute a powerful material platform for analyte induced out-coupling of light at interfaces. The effectiveness of the dynamic nature of complex double emulsions is the result of large changes in the refractive index within the evanescent field region of waveguide sensing devices. We demonstrate the concept by creating a sensor capable of the rapid and sensitive detection of caffeine using a tailor-designed stimuli-responsive surfactant. We also showed the generality of the method for the detection of concanavilin A, an *E. coli* mimic using changes in droplet orientation. The system is compact and operates near real time. The general applicability of both transduction schemes presented herein suggests that dynamic complex emulsions have a significant potential as a broadly deployable transduction material in waveguide-based chemo- and bio-sensing platforms.

Conflicts of interest

There are no conflicts to declare.

Acknowledgements

We are grateful for the support of the National Institutes of Health of General Medical Sciences (Grant No. GM095843). L. Z. acknowledges support from the German Research Foundation (DFG, Grant No. ZE1121/1-1). S.S. was supported by an F32 Ruth L. Kirschstein National Research Service Award. We thank Dr. Joe Walish, Sara Nagelberg, and Prof. Mathias Kolle for helpful discussions.

References

1 W. Lukosz, *Sens. Actuators, B*, 1995, **29**, 37.
2 C. McDonagh, C. S. Burke and B. D. MacCraith, *Chem. Rev.*, 2008, **108**, 400.
3 C. Girard, C. Joachim and S. Gauthier, *Rep. Prog. Phys.*, 2000, **63**, 893.
4 H. Nishihara, M. Haruna and T. Suhara, *Electro-Optics Handbook* 2000.
5 J. Y. Han, in *Proceedings of the 18th annual ACM symposium on user interface software and technology*, ACM, 2005, pp. 115–118.
6 C. S. Burke, A. Markey, R. I. Nooney, P. Byrne and C. McDonagh, *Sens. Actuators, B*, 2006, **119**, 288.
7 L. Reverté, M. Campàs, B. J. Yakes, J. R. Deeds, P. Katikou, K. Kawatsu, M. Lochhead, C. T. Elliott and K. Campbell, *Sens. Actuators, B*, 2017, **253**, 967–976.

8 T. Kondo, W. J. Chen and G. S. Schlau-Cohen, *Chem. Rev.*, 2017, **117**, 860.
9 J. Escorihuela, M. A. González-Martínez, J. L. López-Paz, R. Puchades, A. Maquieira and D. Gimenez-Romero, *Chem. Rev.*, 2014, **115**, 265–294.
10 M. Puyol, M. del Valle, I. Garcés, F. Villuendas, C. Domínguez and J. Alonso, *Anal. Chem.*, 1999, **71**, 5037.
11 C. Lavers, K. Itoh, S. Wu, M. Murabayashi, I. Mauchline, G. Stewart and T. Stout, *Sens. Actuators, B*, 2000, **69**, 85.
12 H. Mukundan, A. S. Anderson, W. K. Grace, K. M. Grace, N. Hartman, J. S. Martinez and B. I. Swanson, *Sensors*, 2009, **9**, 5783.
13 O. Tokel, U. H. Yildiz, F. Inci, N. G. Durmus, O. O. Ekiz, B. Turker, C. Cetin, S. Rao, K. Sridhar and N. Natarajan, *Sci. Rep.*, 2015, **5**, 9152.
14 R. Roy, S. Hohng and T. Ha, *Nat. Methods*, 2008, **5**, 507.
15 M. J. Swann, L. L. Peel, S. Carrington and N. J. Freeman, *Anal. Biochem.*, 2004, **329**, 190–198.
16 D. Maltoni, D. Maio, A. K. Jain and S. Prabhakar, *Handbook of fingerprint recognition*, Springer Science & Business Media, 2009.
17 J.-Y. Yoon and B. Kim, *Sensors*, 2012, **12**, 10713.
18 M. S. Luchansky and R. C. Bailey, *Anal. Chem.*, 2011, **84**, 793.
19 W. Lukosz and K. Tiefenthaler, *Sens. Actuators*, 1988, **15**, 273.
20 C. A. Rowe-Taitt, J. W. Hazzard, K. E. Hoffman, J. J. Cras, J. P. Golden and F. S. Ligler, *Biosens. Bioelectron.*, 2000, **15**, 579.
21 J. Xavier, S. Vincent, F. Meder and F. Vollmer, *NANO*, 2018, **7**, 1.
22 C. F. Carlborg, *et al.*, *Lab Chip*, 2010, **10**, 281.
23 S. J. Tang, S. Liu, X. C. Yu, Q. Song, Q. Gong and Y. F. Xiao, *Adv. Mater.*, 2018, 1800262.
24 C. Lin, C. Liao, Y. Zhang, L. Xu, Y. Wang, C. Fu, K. Yang, J. Wang, J. He and Y. Wang, *Lab Chip*, 2018, **18**, 595.
25 X.-C. Yu, Y. Zhi, S.-J. Tang, B.-B. Li, Q. Gong, C.-W. Qiu and Y.-F. Xiao, *Light: Sci. Appl.*, 2018, **7**, 18003.
26 M. L. Douvidzon, S. Maayani, L. L. Martin and T. Carmon, *Sci. Rep.*, 2017, **7**, 16633.
27 W. Chen, Ş. K. Özdemir, G. Zhao, J. Wiersig and L. Yang, *Nature*, 2017, **548**, 192.
28 Y.-N. Zhang, Y. Zhao, T. Zhou and Q. Wu, *Lab Chip*, 2018, **18**, 57.
29 M. Hossein-Zadeh and K. J. Vahala, *Opt. Express*, 2006, **14**, 10800.
30 L. D. Zarzar, V. Sresht, E. M. Sletten, J. A. Kalow, D. Blankschtein and T. M. Swager, *Nature*, 2015, **518**, 520.
31 Z. Köstereli and K. Severin, *Org. Biomol. Chem.*, 2015, **13**, 9231.
32 T. M. Swager, *Angew. Chem., Int. Ed.*, 2018, **57**, 4248.
33 Y. Zhao, L. Chen and T. M. Swager, *Angew. Chem., Int. Ed.*, 2016, **55**, 917.
34 L. D. Zarzar, J. A. Kalow, X. He, J. J. Walish and T. M. Swager, *Proc. Natl. Acad. Sci. U. S. A.*, 2017, **114**, 3821.
35 Q. Zhang, *et al.*, *ACS Sens.*, 2019, **4**, 180.
36 Q. Zhang, S. Savagatrup, P. Kaplonek, P. H. Seeberger and T. M. Swager, *ACS Cent. Sci.*, 2017, **3**, 309.